III. Electron Diffraction

A. Principles of Diffraction

Diffraction is the spreading of waves around obstacles. One consequence of diffraction is that sharp shadows are not produced. The phenomenon is most pronounced when the wavelength of the radiation is comparable to the linear dimensions of the obstacle. When a beam of light falls on the edge of an object, it will not continue in a straight line but will be slightly bent by the contact, causing a blur at the edge of the shadow of the object. The amount of bending will be proportional to the wavelength.

When a monochromatic beam of light falls on a single edge, a sequence of light and dark bands is produced due to **interference**; and with white light a sequence of colours much like the **Newton colour sequence** appears.

A **diffraction grating** consists of a regular two- or three-dimensional array of objects or openings that scatter light according to its wavelength over a wide range of angles. As these deflected waves interact, they reinforce one another in some directions to produce intense spectral colours. Diffraction arrays that reveal spectral colours in direct sunlight exist on the wings of some beetles and the skins of some snakes. Perhaps the most outstanding natural diffraction grating, however, is the gemstone opal. Electron microscope photographs reveal that an opal has a regular three-dimensional array of equal-size spheres, about 250 nm in diameter, which produce the diffraction.

Huygens showed that every point on a wave front may be regarded as a source of spherical wavelets, thus accounting for the laws of reflection and refraction. **Fresnel** added the hypothesis that the wavelets can **interfere**, and this led to a theory of diffraction.

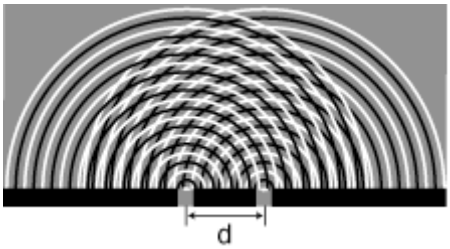

1. Interference

Interference is the term used to describe the interaction of waves. These waves are typically electromagnetic radiation (visible light, x-rays, etc.) or matter waves (electrons, neutrons, etc.), although sound waves also behave this way. Any two (or more) waves whose wavefronts meet interfere with each other, that is, the resultant wave is the sum of the first two. **Constructive interference** occurs when the two initial waves are exactly in-phase - the peaks and troughs of one wave are aligned with the peaks and troughs of the other. **Destructive interference** occurs when the peaks of one wave coincide with the troughs of the other. When two waves of equal amplitude are exactly half a wavelength (π rad or 180°) out of phase, then their resultant wave has zero amplitude - they cancel out!

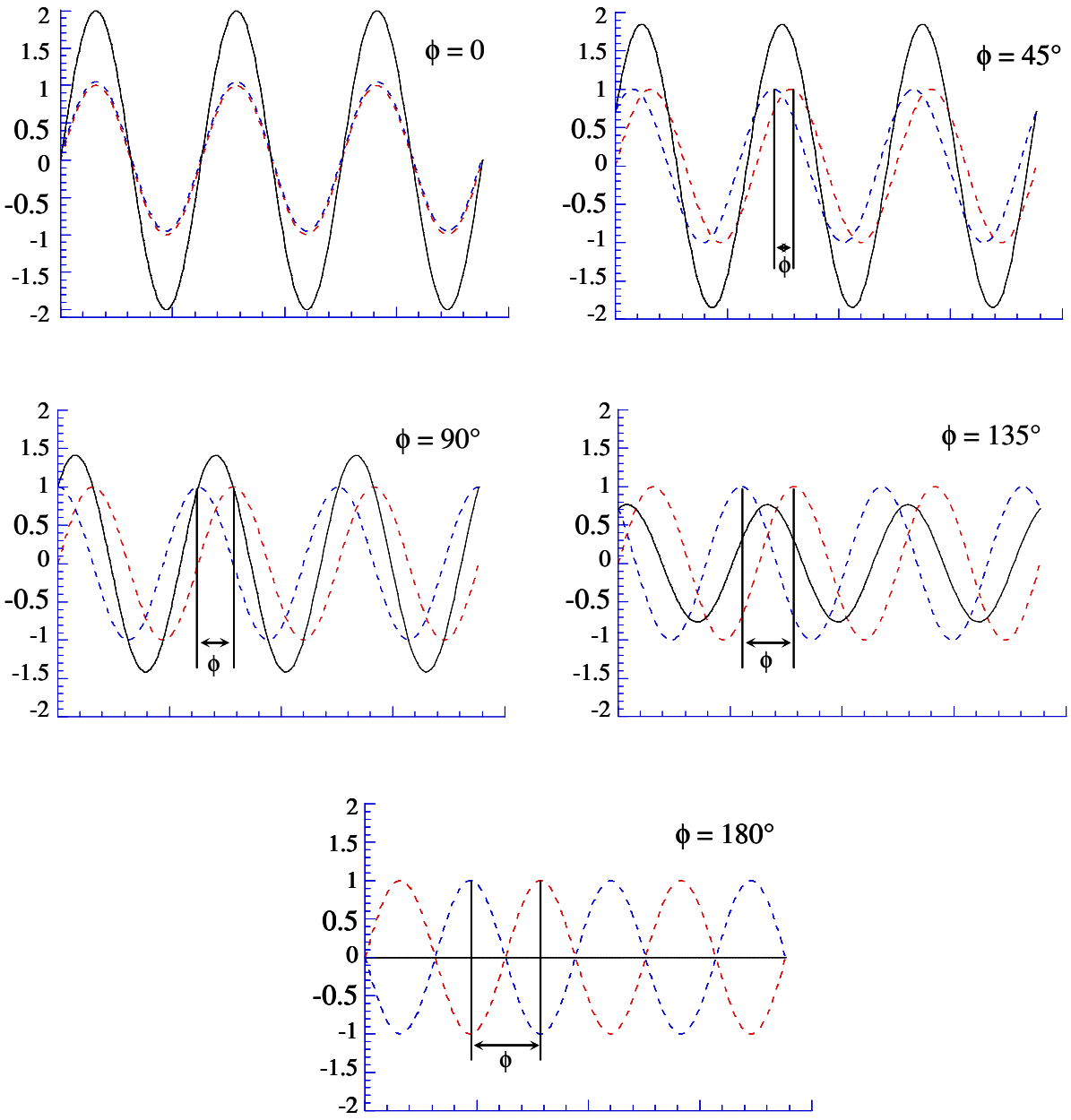

Interference also occurs between two wave trains moving in the same direction but having different wavelengths or frequencies. The resultant effect is a complex wave, and a pulsating frequency, called a **beat**, results when the wavelengths are slightly different.

2. Fraunhofer ($L >> a$) Single Slit Diffraction

Plane waves that pass through a restricted opening emerge as divergent waves. When the opening is less than one wavelength in diameter the emergent wave is nearly spherical. Whenever a beam of light is restricted by holes or slits or by opaque obstacles that block out part of the wave front, some spreading occurs at the edges of geometrical shadows.

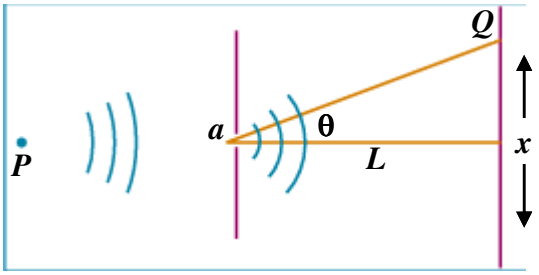

$$I_\theta = I_m\left(\frac{\sin\alpha}{\alpha}\right)^2 \quad where \quad \alpha = \frac{\pi a}{\lambda}\sin\theta$$

The minima occur at

$$\sin\theta = \frac{m\lambda}{a} \quad \text{or} \quad R = \frac{m\lambda L}{\sqrt{a^2 - m^2\lambda^2}} \approx \frac{m\lambda L}{a}$$

where a is the slit width and m is an integer (m = 1, 2, 3...) and R is the distance to the minimum as measured on the screen at Q. The approximation for R assumes $L >> R$.

What is projected onto the screen Q is a pattern similar to the one below. The **width of the pattern is inversely proportional to the slit width**, and when $a = \lambda$, $\theta = 90°$, which indicates that the central bright band fills the entire screen.

From the resulting interference pattern that emerges on the screen at Q, it is possible to calculate the width of the slit by accurately measuring the spacing of the minima on the screen. Thus, **diffraction is a way of linking measurable macroscopic phenomena to microscopic ones.**

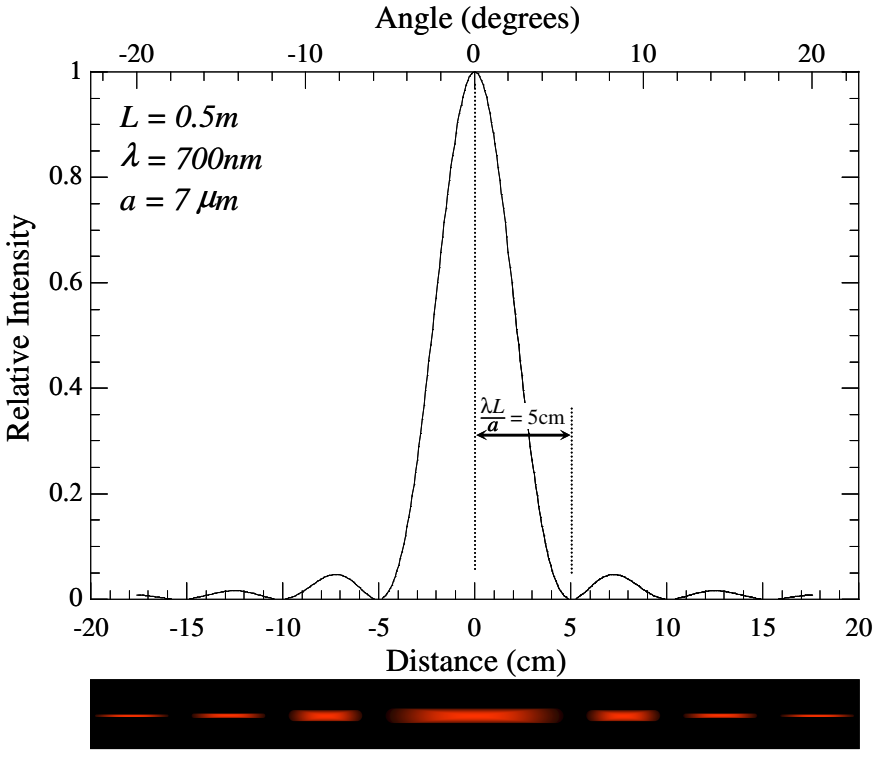

3. Fraunhofer ($L >> a$) Double Slit Diffraction

This experiment is often attributed to **Thomas Young**, who first performed it in 1801 and thus helped prove the wave nature of light. A beam of light is first passed through a single slit as above, and subsequently passed through a double-slit system. The two slits have a width a and are separated by a distance d. The equation which describes the resultant intensity as a function of angle θ is:

$$I_\theta = I_m\left(\frac{\sin\alpha}{\alpha}\right)^2 \cos^2\beta \quad \text{where } \alpha = \frac{\pi a}{\lambda}\sin\theta \quad \text{and } \beta = \frac{\pi d}{\lambda}\sin\theta$$

The second factor on the right-hand side is the **diffraction factor**, while the last factor is the **interference factor**. The result looks similar to single-slit diffraction except the intensity is now modulated by the interference factor. The minima now occur at:

$$d\sin\theta = (m+\tfrac{1}{2})\lambda \quad \text{or} \quad R = \frac{L(m+\tfrac{1}{2})}{\sqrt{d^2/\lambda^2 - (m+\tfrac{1}{2})^2}} \approx \frac{L\lambda(m+\tfrac{1}{2})}{d}$$

and the maxima at *approximately*:

$$d\sin\theta = m\lambda \quad \text{or} \quad R = \frac{L\lambda m}{\sqrt{d^2 - m^2\lambda^2}} \approx \frac{L\lambda m}{d}$$

where m = 0, 1, 2, 3... As with single-slit diffraction, it is possible to link the pattern on the screen to the microscopic nature of the slits. By accurately measuring the spacing of the new maxima or minima on the screen one can calculate the spacing of the slits, d. By measuring the distance between the unmodulated minima, it is also still possible to calculate the width of the slits, as before.

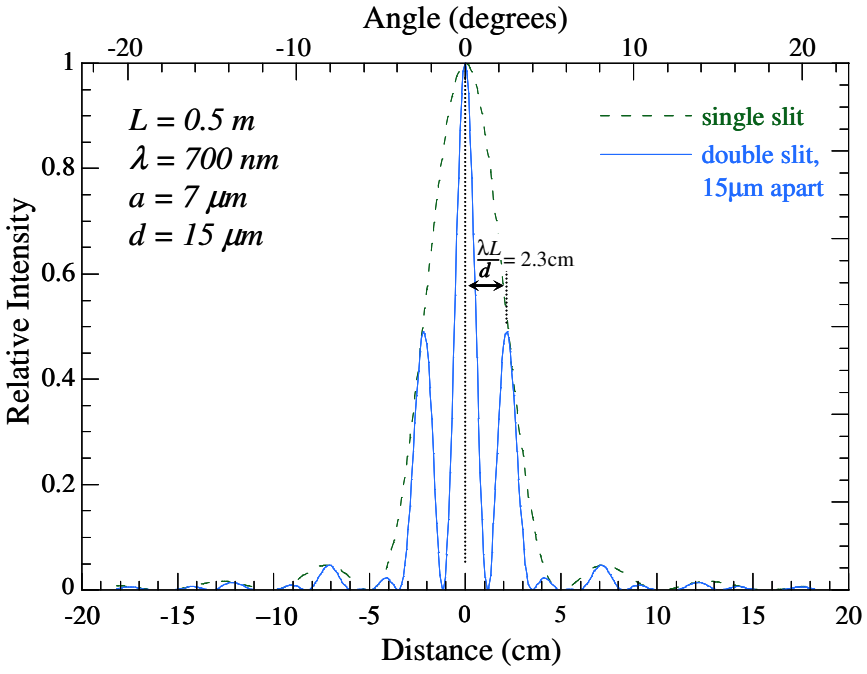

4. Fraunhofer ($L >> a$) Multiple Slit Diffraction

The specific cases of single or double slit diffraction can be generalised for the case of an arbitrary number of slits, n. In this case, the equation of intensity becomes:

$$I_\theta = I_m \left(\frac{\sin^2 \alpha}{\alpha^2} \right) \left(\frac{\sin^2 n\beta}{\sin^2 \beta} \right)$$

The greater the number of slits, the sharper and more intense are the diffraction maxima. The same relationships between d and the maxima/minima spacings still hold and become more accurate the more slits that are included.

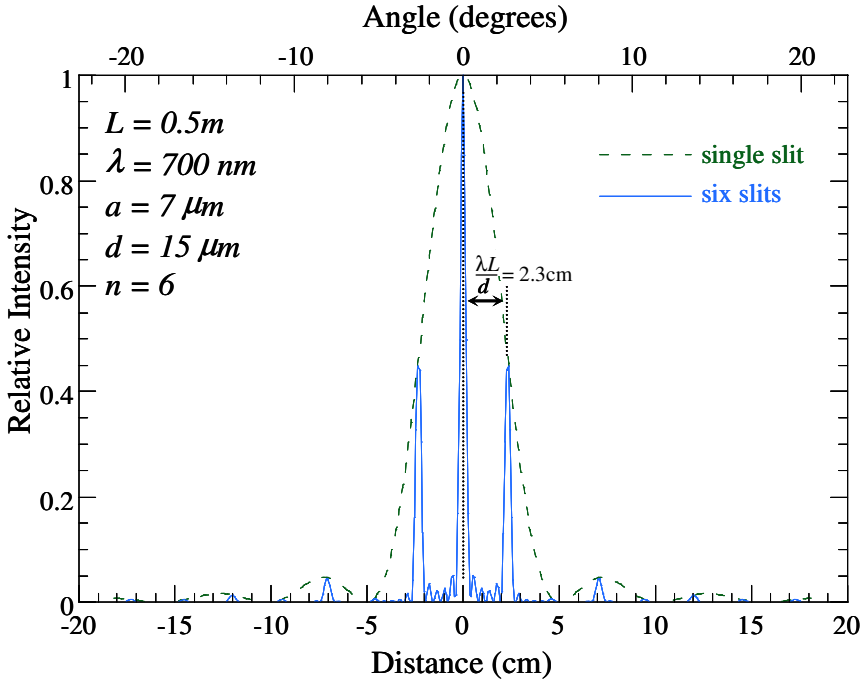

The above graphs have been normalised by a factor of $1/n^2$ for convenience. In reality, the intensity of the diffracted maxima are proportional to n^2; therefore, a **diffraction grating** consisting of thousands of slits can be used to yield very intense – and sharp – diffraction maxima.

5. Fraunhofer ($L >> a$) Circular Aperture Diffraction

When light from a point source passes through a small circular aperture, it does not produce a bright dot as an image, but rather a diffuse circular disc known as **Airy's disc** surrounded by much fainter concentric circular rings.

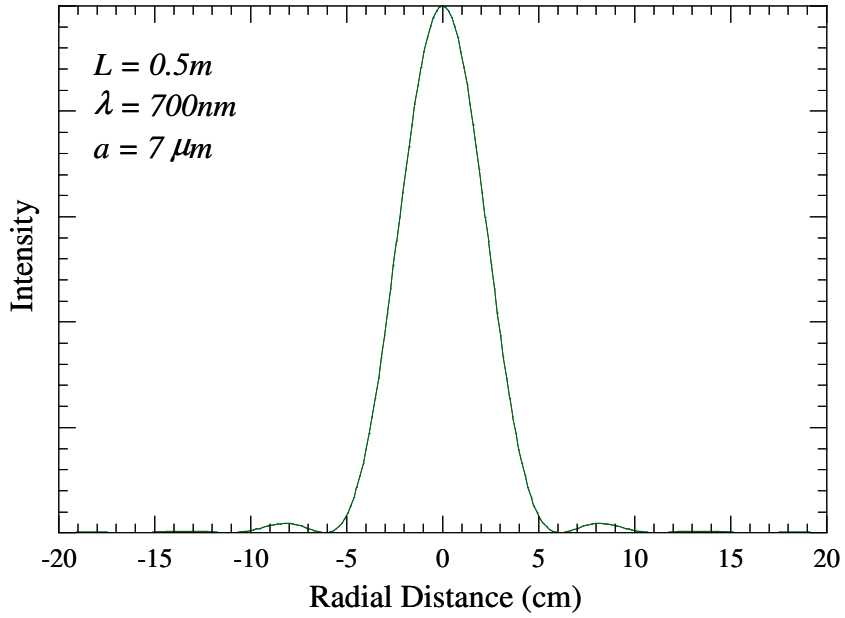

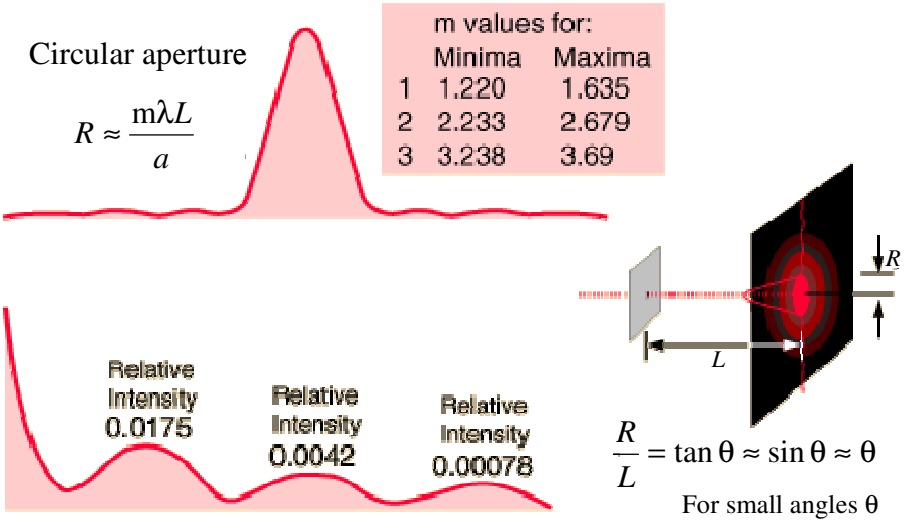

The intensity is given by:

$$I = \frac{\pi^2 a^4}{4}\left(\frac{J_1(\pi aR/L\lambda)}{\pi aR/L\lambda}\right)^2$$

where $J_1(z)$ is a Bessel function of the first kind, so the mimima occur when $J_1(\pi aR/L\lambda) = 0$ (the zeros of the Bessel function of the first kind are 3.831706, 7.0155867, *etc.*) and the maxima correspond to the maxima in the Bessel expression.

B. Quantum Electrodynamics (QED)

From the law of reflection, we expect that the angle of incidence is equal to the angle of reflection, $\theta_i = \theta_f$; however, it is useful to examine that law more closely. Consider the mirror shown in the figure below. The source, S, emits one photon at a time; and a detector is located at P. Let's calculate the chance that a photon from S reaches the detector at P. In order to block the obvious straight path between S and P, we'll put a screen at Q between them.

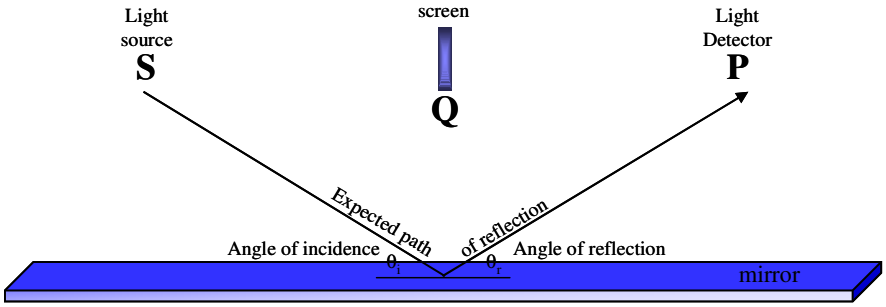

Now, we would expect that all the light that reaches P to have been reflected off the middle of the mirror, where the angle of incidence equals the angle of reflection, and that the far ends of the mirror have no role in the reflection. In fact, there are millions of routes for the photon to go from S to P, as shown below. Let's look at these.

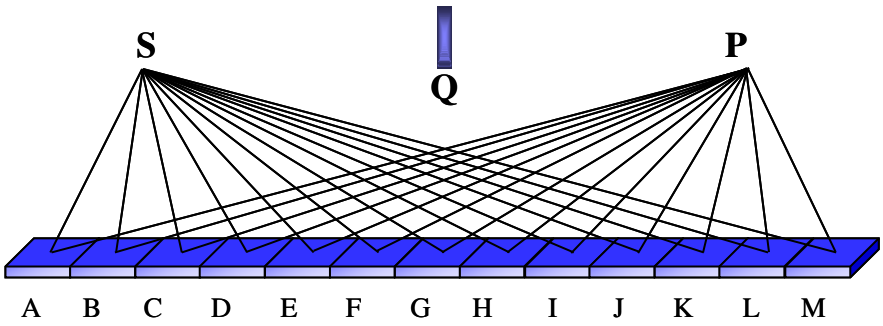

Each of these routes will take a different amount of time for the photon to reach P. The photon will clearly take longer to travel from, for example, S to A to P, than from S to G to P.[†] Because they've been travelling for different times, each photon will be slightly out of phase with its neighbours. If we represent the phase angle by an arrow (vector) whose direction corresponds to the relative phase of the photon (e.g., up = 0°, right = 90°, *etc.*), then we can show graphically both the time required for each path and the relative phase of the photon upon reaching P.

[†] Imagine yourself running from S to P – you'd hardly dash off to A first!

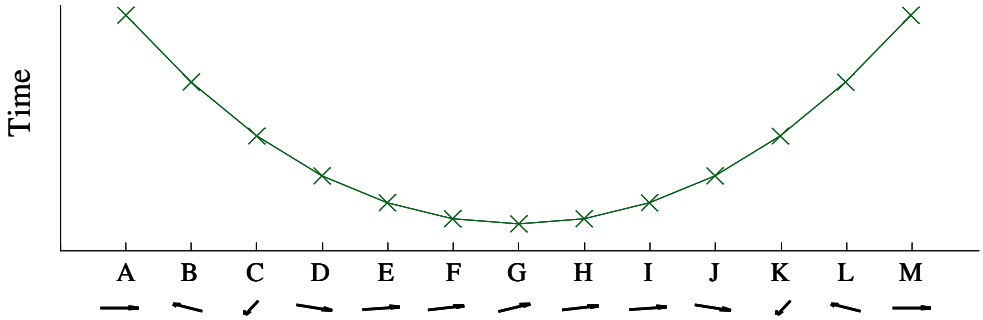

You can think of the arrows as the direction of the hand of a stopwatch when the photon reaches P. By adding up all the arrows, we arrive at a resultant vector which represents the probability of a photon from S arriving at P.[‡]

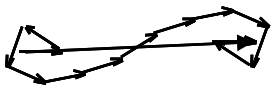

It is apparent that the arrows from the ends of the mirror contribute very little to the overall resultant, and it is the middle section of the mirror which contributes most. This is true because it is in the middle section where the differences between adjacent paths are smallest, so the phase differences are also smallest. The ends of the mirror could easily be chopped off and the reflection would be virtually unaffected, but that does not mean that reflection is not happening there as well! We can test this theory by removing most of the mirror and leaving only a small section way out on the left. What's left of the mirror is now in the wrong place for reflection, you'd think. We'll divide this section up more finely now – fine enough so that there is not much difference in time between adjacent sections.

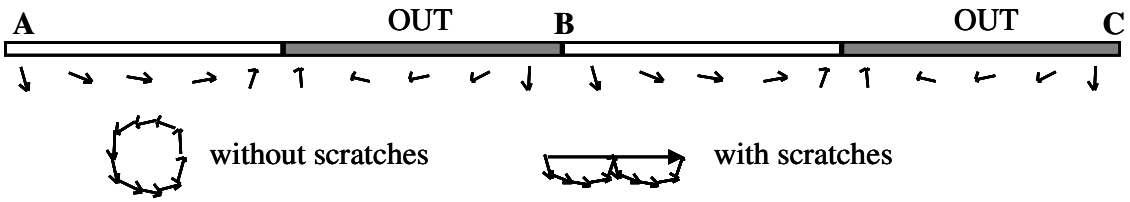

Now we see that some arrows point more or less to the right while others point more or less to the left. If we add all the arrows together, we again find they form more or less a circle and add up zero – no reflection. Now, if just the parts of the mirror where the arrows are pointing to the left are removed, the remaining arrows do indeed add up to a substantial resultant. Reflection does take place! Such a mirror is called a **diffraction grating**.

[‡] Actually, the probability is the square of the magnitude of this vector.

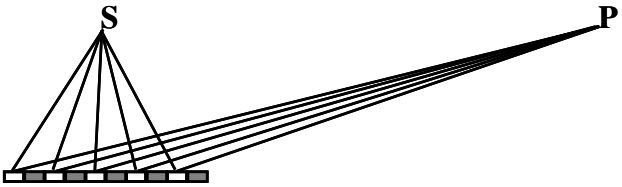

If we designed our grating for red light (say λ = 700nm), it would be no good for blue light. For blue, we'd have to make our cut-away strips closer together because blue light has a higher frequency than red (the stopwatch runs faster); however, by moving the detector to a different angle, the grating made for red light now works for blue. In fact, if you shine white light onto the grating, red light comes out at one angle with orange just next to it followed by all the other colours of the rainbow. The tracks of a CD behave this way. The nominal track separation on a CD is 1.6 μm; so for red light of wavelength 700 nm, this would give a first order diffraction maximum at about 26° (blue is at ≈14°).

Incidentally, this same reasoning can be used to explain the phenomenon of diffraction itself. **Electrons do not simply travel in straight lines**. They *smell out* all neighbouring paths and use a small core of nearby space (all paths which have roughly the same length and so require the same time for the electron). If the gap is wide, then there are many possible linear paths to an off-axis spot, all of which cancel out, and the electron will not be diffracted there. If the gap is too small, then there are only a few possible linear paths to the off-axis spot, too few to cancel out, and some electrons do get there. Ironically, **trying to squeeze electrons too much in order to keep them in a straight line causes them to spread out instead!**

Any periodic reflective surface can behave as a diffraction grating. The scratches in our mirror are several microns apart, and so it is useful for visible light, with wavelengths from ≈400 – 700 nm. A **crystal**, whose atoms are perhaps no more than a few Ångstroms apart, is a natural diffraction grating for **x-ray photons** (for which the imaginary stopwatch runs about 4,000 times faster than for visible light) or **electrons** (for which the imaginary stopwatch runs about 220,000 times faster than for visible light) at various angles, from which can be determined the spacings and exact arrangement of the individual atoms.

C. Geometry of Electron Diffraction

1. Diffraction geometry in the TEM

As we have already seen, electrons, although particles, can behave as waves and so can be diffracted. The wavelength of an electron accelerated by an electric field is given by:

$$\lambda = hc\left(2eVm_oc^2 + e^2V^2\right)^{-1/2}$$

With this relation, it is quite straightforward to show that the wavelength of electrons accelerated by, say, 200 kV (as they are in the JEOL 2100) is 0.025 Å – much smaller than x-ray or typical neutron wavelengths. If such electrons are diffracted from the faces of the cubic crystal thallium chloride, for instance, the angle θ is only 0.186° and the total angular deflection of the electron beam is 0.37°. If a fluorescent screen or photographic film is placed a distance L from the crystal, the diffracted spot will be displaced from the undeviated beam by a distance R such that:

$$R = L\tan 2\theta \approx 2\theta L$$

since for very small θ, tan2θ ≈ 2θ. Combining this relationship with Bragg's law yields:

$$R/L = \lambda/d$$
$$\therefore d = L\lambda/R$$

The factor $L\lambda$ is often referred to as the ***camera constant*** and is generally calibrated experimentally for each microscope. This equation is used to index every kind of electron diffraction pattern.

Electron diffraction differs from x-ray diffraction in a number of ways. **First**, electrons are much less penetrating than x-rays. They are easily absorbed by air (where they can ionise air molecules) which means that the specimen and the recording/detecting device must all be enclosed in vacuum. Transmission electron diffraction patterns can only be obtained with specimens so thin as to be classed as foils (metals) or films. **Second**, electrons are scattered much more intensely than x-rays, so that even a very thin layer gives a strong diffraction pattern in a short time. **Third**, the intensity of electron diffraction decreases with increasing 2θ even more rapidly than for XRD, which means that the entire observable diffraction pattern is limited to an angular range of about ±4° 2θ. We will cover this topic in more detail later on.

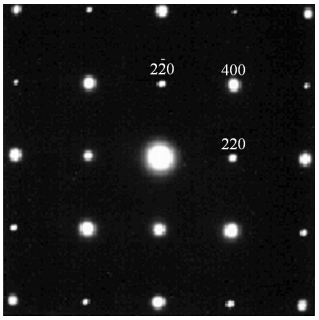

[001] electron diffraction pattern from an fcc crystal.

The figure below shows the geometry of electron diffraction in the TEM. Since the wavelength of electrons is so small (0.025 Å at 200 kV), θ is very small (0.14° for d = 5 Å) and the Bragg equation reduces to $2d\theta = \lambda$. It is also apparent from the figure that $tan2\theta = R/L$, which reduces to $2\theta = R/L$. Combining these two equations yields $Rd = L\lambda$, which is the equation used to index every electron diffraction pattern.

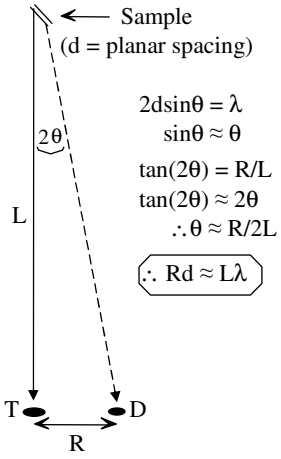

Geometry of electron diffraction in a TEM. *L* is the effective camera length, *T* is the transmitted spot, *D* is the diffracted spot, *R* is the distance between *T* and *D*, and 2θ is the Bragg angle. The angle 2θ is very small due to the small wavelength of the electrons, so Bragg's Law reduces to $2d\theta \approx \lambda$. Additionally, it can be seen that $\tan(2\theta) = R/L$, which reduces to $2\theta \approx R/L$. Combining these two equations yields $Rd \approx L\lambda$.

2. The Structure Factor

The resultant wave scattered by all the atoms in a unit cell is called the structure factor, *F*, because it describes how the atom arrangement affects the scattered beam. Mathematically, it is the sum of all the waves scattered by the individual atoms:

$$F_{(hkl)} = \sum_{1}^{n} f_n e^{2\pi i(hu_n + kv_n + lw_n)}$$

where *f* is the atomic scattering factor (a function of $\sin\theta/\lambda$, tabulated in the International Tables for X-Ray Crystallography) and the summation extends over all the *n* atoms of the unit cell. The coordinates of the n^{th} atom are $(u_n v_n w_n)$ and those of the reflecting plane are (hkl). It is a complex number, combining both the amplitude and phase of the resultant wave. It can be re-written as:[†]

$$F = \sum_{1}^{n} f_n [\cos 2\pi(hu_n + kv_n + lw_n) + i \sin 2\pi(hu_n + kv_n + lw_n)]$$

With this definition in mind, it is fairly easy to prove that:

$$e^{\pi i} = e^{3\pi i} = e^{5\pi i} = -1$$
$$e^{2\pi i} = e^{4\pi i} = e^{6\pi i} = +1$$
$$e^{n\pi i} = e^{-n\pi i} \quad \text{where } n \text{ is any integer}$$
$$e^{n\pi i} = (-1)^n \quad \text{where } n \text{ is an integer}$$

[†] Recall that $e^{ix} = \cos x + i\sin x$

These simple rules enable us to calculate the structure factors for most reflections; however, there are certain special cases in which we are required to use the trigonometric functions instead, *e.g.*, if $(hu_n+kv_n+lw_n) \neq 0, ½, 1...)$.

Now let's look at a real crystal – the simple case of NaCl. This crystal has face-centred symmetry and, because it consists of two different ions, can be described as two interpenetrating fcc lattices offset from each other by (½ 0 0); therefore, there are eight ions per unit cell. The coordinates are:

Na: (0 0 0) (½ ½ 0) (½ 0 ½) (0 ½ ½)
Cl: (½ ½ ½) (½ 0 0) (0 ½ 0) 0 0 ½)

$$F = f_{Na}e^{2\pi i(0)} + f_{Na}e^{2\pi i\left(h/2+k/2\right)} + f_{Na}e^{2\pi i\left(h/2+l/2\right)} + f_{Na}e^{2\pi i\left(k/2+l/2\right)} + f_{Cl}e^{2\pi i\left(h/2+k/2+l/2\right)} + f_{Cl}e^{2\pi i\left(h/2\right)} + f_{Cl}e^{2\pi i\left(k/2\right)} + f_{Cl}e^{2\pi i\left(l/2\right)}$$

$$F = f_{Na}\left(1 + e^{\pi i(h+k)} + e^{\pi i(h+l)} + e^{\pi i(k+l)}\right) + f_{Cl}\left(e^{\pi i(h+k+l)} + e^{\pi ih} + e^{\pi ik} + e^{\pi il}\right)$$

We can factor out an $e^{\pi i(h+k+l)}$ from the Cl term and obtain:

$$F = f_{Na}\left(1 + e^{\pi i(h+k)} + e^{\pi i(h+l)} + e^{\pi i(k+l)}\right) + f_{Cl}e^{\pi i(h+k+l)}\left(1 + e^{-\pi i(k+l)} + e^{-\pi i(h+l)} + e^{-\pi i(h+k)}\right)$$

Now, because $e^{n\pi i} = e^{-n\pi i}$, the signs of the exponents in the Cl term can be changed:

$$F = f_{Na}\left(1 + e^{\pi i(h+k)} + e^{\pi i(h+l)} + e^{\pi i(k+l)}\right) + f_{Cl}e^{\pi i(h+k+l)}\left(1 + e^{\pi i(k+l)} + e^{\pi i(h+l)} + e^{\pi i(h+k)}\right)$$

This expression can be re-grouped:

$$F = \left(1 + e^{\pi i(h+k)} + e^{\pi i(h+l)} + e^{\pi i(k+l)}\right)\left(f_{Na} + f_{Cl}e^{\pi i(h+k+l)}\right)$$

Here, the first set of parentheses corresponds to the face centring, whereas the second term corresponds to the *basis* of the unit cell – the one Na^+ and one Cl^- associated with each lattice point. The first part vanishes if h, k, and l are mixed odd and even, otherwise it is equal to 4. For unmixed indices (all odd or all even),

$$F = 4\left(f_{Na} + f_{Cl}e^{\pi i(h+k+l)}\right)$$
$$= 4(f_{Na} + f_{Cl}) \quad \text{if } (h+k+l) \text{ is even}$$
$$= 4(f_{Na} - f_{Cl}) \quad \text{if } (h+k+l) \text{ is odd}$$

Introducing a second atom type has not eliminated any reflections allowed, but it has decreased the intensity of some. For example, the (111) reflection now involves the difference, rather than the sum, of the scattering powers of the two ions. This result is independent of which way round the Cl^- and Na^+ are labelled in the unit cell. It is the *relative* position of the atoms which is important.

3. Spot patterns

The nature of the diffraction pattern is in indication of the number of grains contributing towards the pattern or the crystallinity of the specimen. A single crystal will give rise to a spot pattern, whereas diffraction from several crystals causes several overlapping spot patterns in which all the spots can be seen to lie along Debye rings. In the extreme case of hundreds of crystals contributing to the pattern, then the resulting spots are so closely spaced that they are no longer identifiable and merge into continuous rings (Debye rings). An amorphous sample results in no regular diffraction pattern.

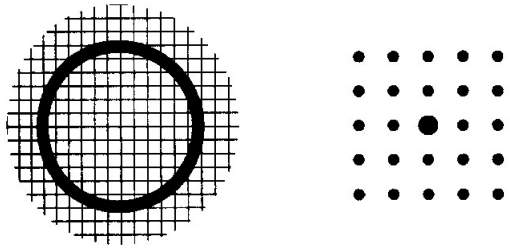

Single, perfect crystal

Diffraction pattern is regular array of dots

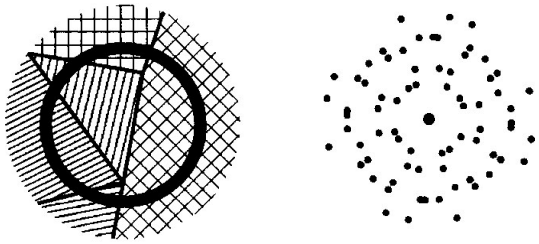

Small number of grains (crystals) with different orientation.

Diffraction pattern is discrete spots, each lying on a Debye ring

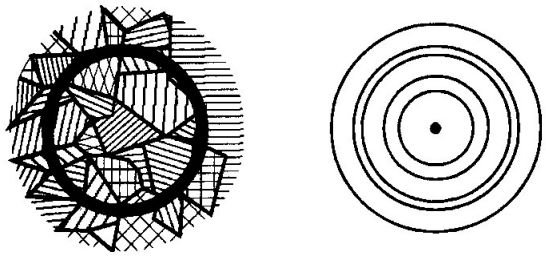

Large number of randomly oriented grains.

Diffraction pattern is continuous Debye rings

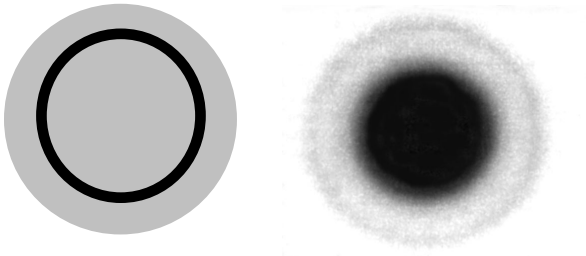

Amorphous material

No distinct diffraction pattern

4. The reciprocal lattice

The concept of the reciprocal lattice is one of convenience, as all spacings in a diffraction pattern are inversely proportional to the corresponding real spacing. It is constructed by converting each real-lattice plane (*hkl*) into a point at a distance $g = 1/d_{hkl}$ from the origin of the reciprocal lattice (d_{hkl} is the real-lattice spacing of the (*hkl*) planes) along a direction perpendicular to (*hkl*). Some planes may not appear in the reciprocal lattice if they are forbidden by the extinction rules for the real-lattice crystal symmetry. If the real lattice has dimensions a_o, b_o, c_o, then the reciprocal lattice's dimensions are $a^* = 1/a_o$, $b^* = 1/b_o$, $c^* = 1/c_o$; and a^* is normal to b_o and c_o, b^* is normal to a_o and c_o, and c^* is normal to a_o and b_o. The reciprocal lattice of an fcc crystal is a bcc one (and vice versa). Points in the reciprocal lattice are not "points" in the mathematical sense, but have some shape and size associated with them inversely proportional to the dimensions of the crystal or feature being examined (shape factor).

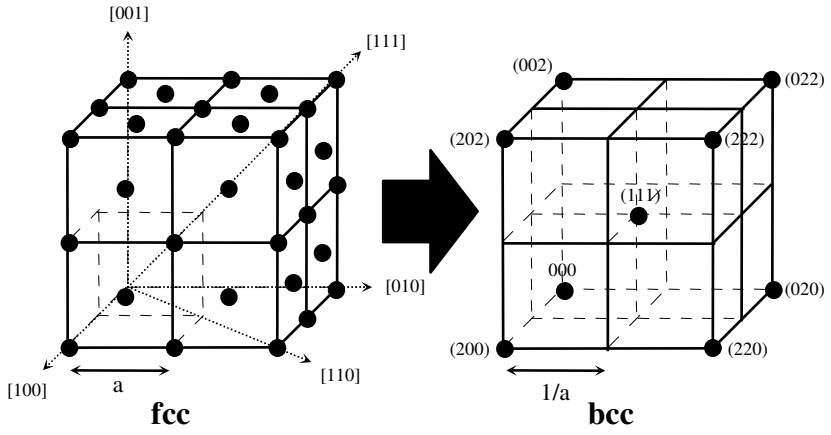

The reciprocal of an fcc real lattice is bcc.

5. The Ewald (or Reflecting) Sphere

The Ewald sphere is another geometrical convenience for calculating when diffraction occurs for some arbitrary planes. A hypothetical sphere is centred on the point of electron scattering in the specimen and has a radius of $1/\lambda$. Because the λ of electrons accelerated by, say, 100 kV, is only 0.037 Å, the radius of the sphere is 27 $Å^{-1}$. The surface of this sphere can easily intersect more than one point in the reciprocal lattice, and so many spots can appear in a diffraction pattern. The size of the sphere is a major advantage of electron diffraction over, say, x-ray diffraction (XRD), which can excite only one Bragg reflection at a time. The Cu Kα radiation often used in XRD has λ = 1.54056 Å, with the Ewald sphere radius only 0.65 $Å^{-1}$. Thus, the radius of the sphere is over 40 times bigger for 100 kV electrons, and the volume of the sphere is over 72,000 times bigger!

Using the Ewald sphere construction to predict which diffraction spots will occur is equivalent to the Bragg condition. The intersection of the sphere with successive lattice planes results in higher-order Laue zones (HOLZ). The zero-order Laue zone (ZOLZ) is typically used most often for indexing patterns, as most information is there and the first-order Laue zone (FOLZ) is often too far away to be imaged.

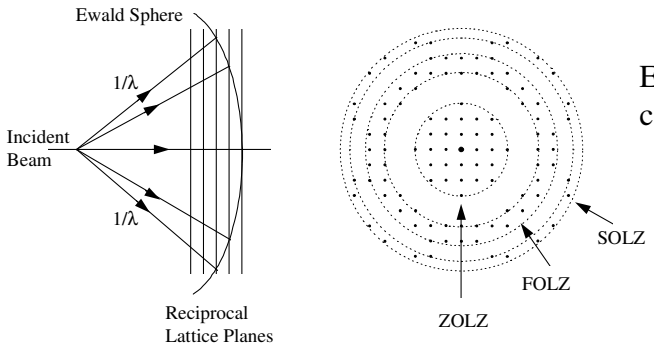

Ewald sphere construction.

6. Diffraction Theory

There are two sets of theory and equations which explain electron diffraction; kinematic theory and dynamical theory. The **kinematic** theory is simpler and relies upon a few approximations and assumptions. First, the intensity of diffracted spots must be much smaller than the intensity of the transmitted beam. Second, it assumes that electrons scatter only once in the specimen and do not subsequently interact in any way with each other or undiffracted electrons. This is approximately the case for exceptionally thin specimens or when the geometry is far from the Bragg angle. The **dynamical** theory, on the other hand, accounts for absorption by thick specimens and the multiple interactions of electrons which scatter and can be re-scattered. The intensity of the diffracted waves can be almost as large as that of the transmitted waves. Dynamical scattering makes it much more difficult to calculate the intensity of diffracted spots, as events like double diffraction can redistribute diffracted intensity from one spot to another - even into forbidden reflections.

7. Double Diffraction

Double diffraction is a dynamical effect whereby electrons which have been Bragg diffracted by one set of planes now satisfy the Bragg condition for another set of planes, and so are diffracted twice. The figure below shows two DP's, (a) has been calculated kinematically, and (b) is an actual experimental DP obtained from a JEOL 200CX (200 kV). The difference in intensities is obvious, and a few reflections which occur in (b) are not predicted by (a). For any double-diffracted spot, there must be a diffraction path which allows it. For example, the (002) spot which occurs in (b) is forbidden by the extinction rules and so does not appear in (a); however, since both $(1\,\bar{1}\,1)$ and $(\bar{1}\,1\,1)$ are allowed, and $(1\,\bar{1}\,1)+(\bar{1}\,1\,1)=(002)$, there is a legitimate route for double diffraction, and the (002) spot appears. A short, visual way of determining if a double diffraction route exists is to overlay the simulation (tracing it on acetate helps) on the experimental DP and aligning the simulated transmitted spot onto each real diffraction spot. If the simulation contains a diffracted spot which coincides with an extra spot on the experimental DP, then there is a route for double diffraction. Essentially, this is the same as turning each diffracted beam into another transmitted beam, which is exactly what double diffraction is.

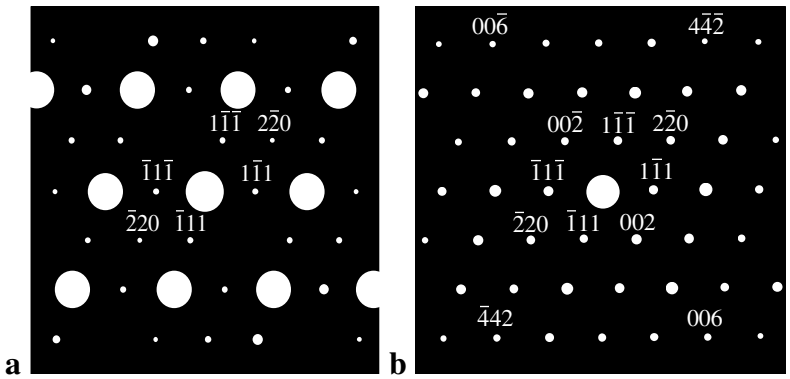

(a) Kinematic simulation and (b) experimental DP of fcc $Nd_2Hf_2O_7$ with the beam parallel to [110] (zone axis = [110]).

8. Kikuchi Lines

Kikuchi lines, first observed by S. Kikuchi in 1928, are another consequence of the dynamical theory. When electrons are incident on a sample, some of the electrons are inelastically scattered (they lose energy). Since more scattered electrons lose small amounts of energy than large amounts, the wavefront of the incident beam is biased in the forward (downward) direction. Many electrons are scattered through an angle α and now satisfy the Bragg condition for an arbitrary set of planes.

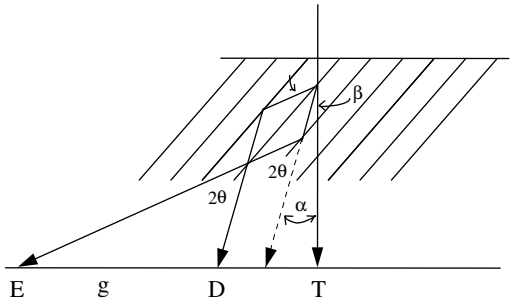

These electrons end up at E. Fewer electrons scatter through the larger angle β and are subsequently diffracted by the same planes to D. Since more electrons are re-directed towards E than are lost in going to D, the result is a bright line at E and a dark line at D. T is the transmitted spot and g is the spot corresponding to the reflecting planes (*hkl*). When the sample is oriented exactly at the Bragg condition for (*hkl*), D passes through the centre of T and E passes through g. The distance between E and g is known as the deviation parameter and is a very accurate way of measuring the angular deviation from the exact Bragg condition.

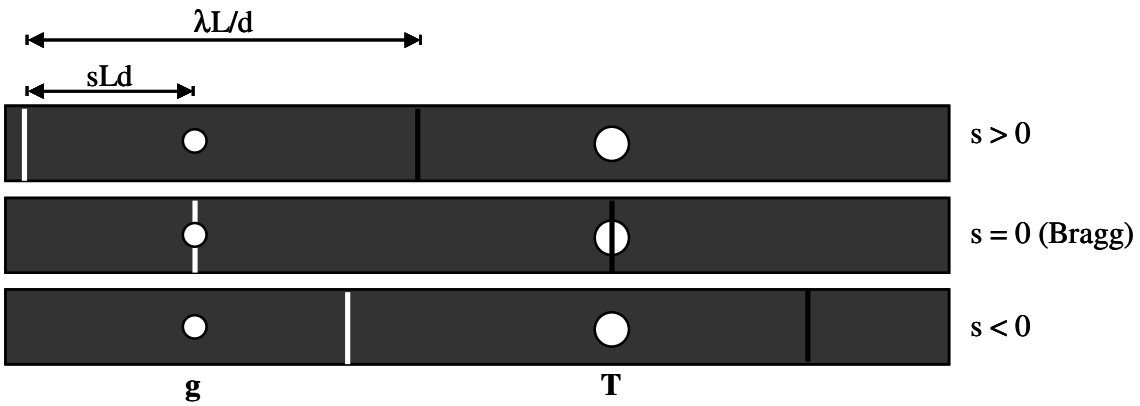

In reality, the bright and dark lines observed on flat DP negatives are hyperbolic intersections of the film with cones (Kikuchi or Kossel cones), one bright and one dark. The excess line is always further away from T than the deficit line (for $s \geq 0$) since $\alpha < \beta$.

Kikuchi lines are very useful in orienting the crystal precisely in the TEM. When the specimen is tilted, the Kikuchi lines move as if they were attached to the bottom of the crystal. The various diffracted spots never move, they just appear and disappear as the angle changes; but Kikuchi lines move with the specimen. Following them is a handy way to tilt systematically in order to navigate from one zone axis to another or to find appropriate two-beam conditions (where only one set of planes Bragg diffracts) for defect analysis.

Kikuchi lines are only observable if the specimen is thick enough to generate sufficient intensity of scattered electrons. In a very thin specimen the lines will be too weak to distinguish from the background. As thickness increases, Kikuchi lines and then bands are observed until finally total absorption occurs and nothing is visible.

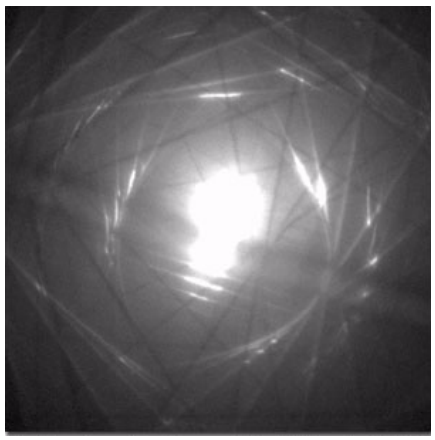

9. Crystal Shape Factor

Since all distances (lengths) in reciprocal space are 1/(real-space distances), the *shape* of the TEM specimen has an effect on the shape of the reciprocal lattice points. A disk-shaped TEM sample is very thin (about 100nm in the *z* direction) but has a comparatively large area (*x* and *y* directions). Consequently, a disk-shaped specimen will produce electrons distributed along a rod

passing through the reciprocal lattice point. The rods, called ***rel rods***, are thin in *x* and *y* but thick in *z*.

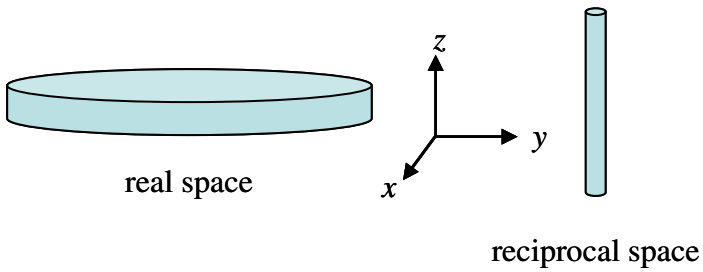

They are also longer for thinner crystals. The fact that reciprocal lattice points are, in fact, three-dimensional rods and not mathematically defined zero-dimensional points makes it possible to get diffracted intensity even when the Bragg condition is not exactly satisfied. The ***deviation parameter***, **s**, is defined as the deviation from the exact Bragg condition where the Ewald sphere cuts the rel rod.

10. Indexing Diffraction Patterns

The method of indexing diffraction patterns (labelling the spots with appropriate *hkl*'s) varies according to what is known of the specimen (crystallography) and diffraction conditions (camera length and voltage). Typically, an experimentalist will have a fairly good idea of what phase or possible phases produced the pattern and a reasonable knowledge of L and λ (the product $L\lambda$ is often referred to as the ***camera constant***). In such a case, the work is much simplified; however, if the crystallography is completely unknown, the procedure is complex and requires a lot of trial and error.

To begin indexing a diffraction pattern (DP) such as the one below, a list of R spacings is required. A good idea is to put a ruler across the negative and measure the space across an entire systematic row of spots, and take an average for the space between each spot. The corresponding *d*-spacings can then be calculated as $L\lambda/R$. These *d*-spacings can be checked against a list of *d*-spacings for various possible phases. A good start is the JCPDS card files, which usually contain sufficient crystallographic information to calculate *d*-spacings. Since more reflections are possible in electron diffraction by ***double diffraction*** than occur by XRD, the JCPDS cards may not list all the *d*-spacings observed in the DP, and the remaining spacings must be calculated. There are a few simple equations for calculating *d*-spacings of planes in various crystal systems. In the case of a cubic crystal,

$$\frac{1}{d^2} = \frac{h^2 + k^2 + l^2}{a^2}$$

Once generic *hkl*'s are found, they must be made systematic.

In the case of the DP below, $|\mathbf{g_1}| = |\mathbf{g_3}|$ and both correspond to a *d*-spacing of 6.14 Å, matching the {111} of fcc $Nd_2Hf_2O_7$. The magnitude of vector $\mathbf{g_2}$ corresponds to d = 3.76 Å, matching {220} of $Nd_2Hf_2O_7$. From the DP, it is clear that $\mathbf{g_1} + \mathbf{g_3} = \mathbf{g_2}$, and this must be the case for the

hkl's. With this rule, the spots are made systematic by indexing $\mathbf{g_1}$ as $(1\bar{1}\,\bar{1})$, $\mathbf{g_2}$ as $(2\bar{2}0)$, and $\mathbf{g_3}$ as $(1\,\bar{1}\,1)$. In this way, $\mathbf{g_1} + \mathbf{g_3} = (1\bar{1}\,\bar{1}) + (1\,\bar{1}\,1) = (2\bar{2}0) = \mathbf{g_2}$. Every other spot in the pattern is now determined by similar vector addition.

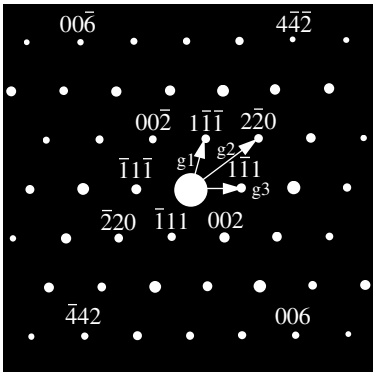

Diffraction pattern from fcc $Nd_2Hf_2O_7$.

Since the camera constant is typically only approximately known, the ratios of *d*-spacings should be checked to ensure that they match those calculated from the JCPDS card. Even if the absolute value of the *d*'s is slightly off, the ratio of *d*'s should be very nearly an exact match. As an additional check, the angles between each plane should be measured to ensure that they are correct. For cubic crystals, the angle ϕ between two planes (two plane normals), $h_1k_1l_1$ and $h_2k_2l_2$, is given by:

$$\cos\phi = \frac{h_1h_2 + k_1k_2 + l_1l_2}{\sqrt{\left(h_1^2 + k_1^2 + l_1^2\right)\left(h_2^2 + k_2^2 + l_2^2\right)}}$$

11. Zone Axis Identification

If the planes in a diffraction pattern have been indexed correctly, then the zone axis [mnp] is defined as the direction which they all have in common. The ***g*** vectors of all the planes must be perpendicular to this direction, *i.e.*, *[hkl] • [mnp] = 0*. It is determined by finding two spots, $h_1k_1l_1$ and $h_2k_2l_2$, which are not on the same systematic row. Then, $m = k_1l_2 - k_2l_1$, $n = l_1h_2 - l_2h_1$, $p = h_1k_2 - h_2k_1$. A simple way is to write down the plane indices in two columns and strike out the first and last digits in each column. Then, a simple cross-multiplication gives the correct result. Sometimes, a high-index direction will be calculated, *e.g.*, [220], as in this case. For crystallographic *directions*, one can legitimately multiply through by any number and still arrive at an equivalent direction. Multiplying [220] through by ½ yields [110], which is the lowest index possible for this direction and so is reported as the direction of the zone axis (the *magnitude* of vectors [220] and [110] are different, but their *directions* are crystallographically identical).

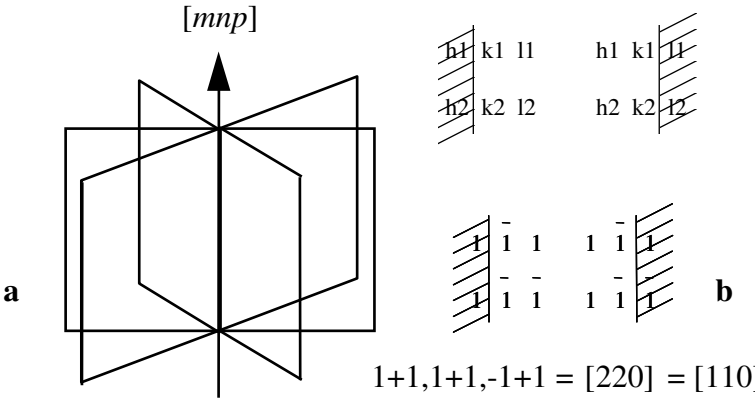

(a) Generic illustration of a zone axis.
(b) Determination of the zone axis of the diffraction pattern in the figure above.

$1+1, 1+1, -1+1 = [220] = [110]$

Of course, this is exactly equivalent to taking the cross product of the two **g** vectors:

$$\det\begin{vmatrix} i & j & k \\ 1 & \bar{1} & 1 \\ 1 & \bar{1} & \bar{1} \end{vmatrix} = i(1+1) - j(-1-1) + k(-1+1) = [220] = [110]$$

The Weiss zone law says that for any plane (*hkl*) contributing to a DP along a given zone axis [*mnp*], then:

$$mh + nk + pl = 0$$

More formally, this rule takes the form of a dot product:

$$\mathbf{g} \bullet \mathbf{r} = \mathbf{0}$$
$$(hkl) \bullet [mnp] = 0$$
$$|hkl| \times |mnp| \cos\theta = 0$$
$$\therefore \cos\theta = 0 \quad \therefore \theta = 90°$$

12. Convergent Beam Electron Microscopy (CBED)

CBED is a powerful tool for probing the crystallography of a small specimen as well for analysing local strains and thicknesses. Conventional diffraction is performed using nearly-parallel electron beams (parallel illumination), and so gives rise to diffraction *spots*. The CBED technique involves focusing the incident illumination down to a fine point, and so yields diffraction discs. Because of the extreme intensity of the focused incident beam, the specimen used must be very stable against the radiation. The specimen will become very hot in the region of the fine probe, and so cooling is generally required to prevent thermal diffuse scattering from obscuring the fine detail within the discs. For the same reason, a very high vacuum system is required to prevent dirt (mostly carbon) from being deposited on the specimen surface. Additionally, the tiny region examined must be defect-free and, if crystallographic information is required, of uniform thickness. Clearly, CBED is not a trivial operation, and the interpretation of CBED patterns is no less difficult! From CBED images it is possible to obtain local specimen thickness (useful when, *e.g.*, determining defect densities), lattice parameters, and crystal structure (even a full space group determination).